Strain relaxation in silicon-germanium microstructures observed by resonant tunneling spectroscopy

A. Zaslavsky
Division of Engineering, Brown University, Providence, Rhode Island 02912

K. R. Milkove and Y. H. Lee
T.J. Watson Research Center, IBM Research, Yorktown Heights, New York 10598

B. Ferland
Division of Engineering, Brown University, Providence, Rhode Island 02912

T. O. Sedgwick
SiBond L.L.C., Hudson Valley Research Park, Hopewell Junction, New York 12533

(Received 10 July 1995; accepted for publication 13 October 1995)

We have measured the resonant tunneling current–voltage $I(V)$ characteristics of strained p-Si/Si$_{1-x}$Ge$_x$ double-barrier microstructures ranging from 1.0 to 0.1 μm in lateral extent. The bias spacing between resonant current peaks in the $I(V)$ reflects the energy separation of the Si$_{1-x}$Ge$_x$ quantum well subbands, which is partially determined by the strain. As the lateral size of the structures decreases, we observe consistent shifts in the $I(V)$ peak spacing corresponding to strain energy relaxation of ~30% in smaller structures. An additional $I(V)$ fine structure is observed in the 0.1 μm device, consistent with lateral quantization due to nonuniform strain.

Heterostructures in lattice-mismatched epitaxial materials offer interesting possibilities of tailoring the electronic properties of semiconductor devices.[1] In a bulk lattice-mismatched heterostructure with translational invariance in the plane, the strain is biaxial and uniform. As long as the strained layer remains below the critical thickness h_c to avoid dislocation formation, the effect of strain on the band structure can be calculated explicitly.[2] In microstructures like quantum wires or dots, however, the lateral extent D of the strained material may be comparable to h_c, giving rise to nonuniform, spatially varying strain distributions[3,4] and making the electronic properties difficult to predict.[5] This issue is particularly significant because the active regions of modern semiconductor devices are pushing into the deep submicrometer range.

In our letter we have focused on the scientifically and technologically interesting strained Si/Si$_{1-x}$Ge$_x$ heterostructures.[6] The epitaxial Si$_{0.75}$Ge$_{0.25}$ layers, strained due to a lattice mismatch of -1% with respect to the Si substrate, are incorporated into the active region of a p-Si/Si$_{1-x}$Ge$_x$ double-barrier resonant tunneling diode (RTD).[7–10] The $I(V)$ characteristics of Si/Si$_{1-x}$Ge$_x$ RTDs reflect the alignment of the two-dimensional (2D) subbands in the SiGe quantum well and the occupied hole states in the emitter electrode, with the lowest-lying heavy-hole (HH$_0$) and light-hole (LH$_0$) subbands giving rise to well-resolved current peaks in the $I(V)$. Since the HH$_0$–LH$_0$ subband energy separation contains a large strain-induced contribution,[2,11] the $I(V)$ peak spacing is an experimentally accessible indication of strain in the structure. In the measured $I(V)$ characteristics of submicrometer RTDs, we observe an unambiguous reduction of HH$_0$–LH$_0$ energy separation corresponding to strain relaxation. Estimating the strain contribution to subband energy separation in the simplest possible manner, we find that the original strain due to the -1% Si/Si$_{0.75}$Ge $_{0.25}$ lattice mismatch is relaxed in small $D=0.25$ μm microstructures by nearly a third. Finally, in the smallest, $D\approx0.1$ μm device, we observe an additional structure in the $I(V)$ line shape that we tentatively attribute to strain-induced lateral quantization of the 2D subbands.

Our microstructures were fabricated of p-Si/Si$_{1-x}$Ge$_x$ RTD material grown at $T=550-600$ °C by atmospheric pressure chemical vapor deposition (CVD) on a p^+-Si substrate.[12,13] The undoped active region consists of a narrow -35 Å Si$_{0.75}$Ge$_{25}$ well clad by -45 Å Si barriers. The active region is, in turn, sandwiched between undoped -100 Å thick Si$_{0.75}$Ge$_{0.25}$ layers and then -100 Å Si$_{1-x}$Ge$_x$ layers in which the Ge content is graded down to pure Si and the doping is gradually increased to match the p^+-Si substrate and top contacting layers. Two-terminal RTDs were fabricated by optical ($D\geqslant3$ μm) and electron-beam (1.0 μm$\geqslant D\geqslant0.1$ μm) lithography, followed by Ti–Al contact metal evaporation, liftoff, low-damage reactive ion etching of the device mesa, SiO$_2$ deposition at $T=300$ °C by plasma-enhanced CVD, dielectric planarization and etch-back, and finally contact pad evaporation.[14] The etching of the microstructure mesa creates a free surface that should result in partial strain relaxation in SiGe layers. A schematic cross-sectional diagram together with an SEM micrograph of a $D=0.3$ μm device prior to contact pad evaporation is shown in Fig. 1(a). It should be noted that because the mesa etch undercut and angled sidewalls the effective lateral size of the RTD is somewhat different from the contact metal pad in Fig. 1(a)—from SEM cross sections we estimate the difference not to exceed ±500 Å.

The $I(V)$ curve of a large device at $T=4.2$ K is shown in Fig. 1(b). The current peaks at $V_p^{\mathrm{HH}}=0.151$ V and $V_p^{\mathrm{LH}}=0.313$ V correspond to tunneling through HH$_0$ and LH$_0$

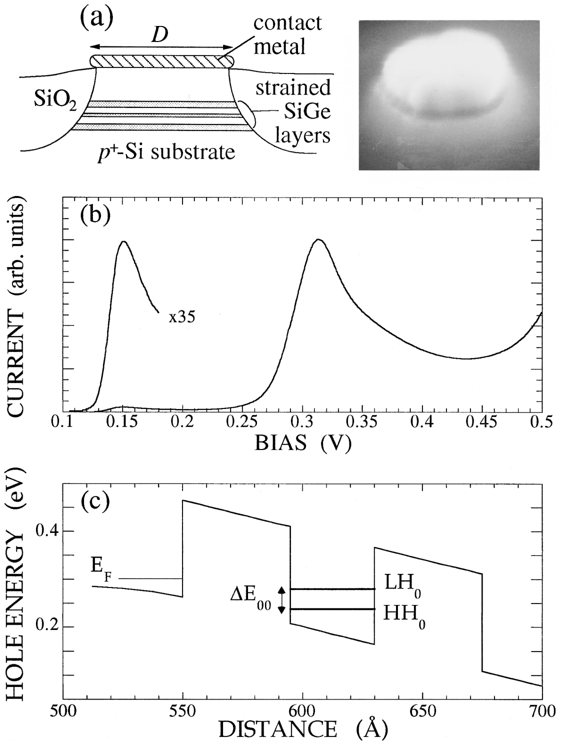

FIG. 1. (a) Schematic cross-sectional illustration of a double-barrier resonant tunneling microstructure and SEM photograph (top view) of a 3000 Å device. (b) $I(V)$ characteristics of a large device at $T=4.2$ K, with a ×35 expanded view of the V_p^{HH} peak. (c) Schematic potential distribution over the double-barrier structure at $V=0.3$ V, showing the lowest-lying heavy-hole (HH$_0$) and light-hole (LH$_0$) subbands and the HH$_0$–LH$_0$ energy separation ΔE_{00}.

subbands with peak-to-valley ratios exceeding 2:1 and 3:1, respectively (comparable to the best results in silicon-based structures [10,13]). The observed $I(V)$ characteristic can be understood within the well-known sequential tunneling model.[15] In the strained Si$_{1-x}$Ge$_x$ emitter, the strain splits the HH and LH band edges,[11,13] so only HH states are occupied at $T=4.2$ K. When the applied bias lines up available 2D states in the quantum well with the emitter, holes can tunnel resonantly into the well, conserving both E and $k_\perp$. By combining a calculation of the subband energies with the self-consistent potential distribution over the device, shown in Fig. 1(c) for a bias of $V=0.3$ V,[16] one obtains the expected threshold and peak bias values for the $I(V)$ peaks (see Ref. 13 for a detailed description). Conversely, the HH$_0$–LH$_0$ peak spacing can be converted to subband energy separation ΔE_{00}. In lattice-matched III–V RTD quantum wells,[17,18] ΔE_{00} arises from the difference in the heavy and light-hole effective masses m^*, but in Si$_{1-x}$Ge$_x$ quantum wells of our devices the strain also contributes to it.[19]

The $I(V)$ characteristics of three RTD microstructures with $D=1.0$, 0.5, and 0.25 μm are shown in Fig. 2. The overall $I(V)$ line shape is retained, with very good peak-to-valley ratios down to $D=0.2$ μm indicating minimal surface damage. As D decreases the current peaks shift: the V_p^{LH} peak moves to lower bias, while the V_p^{HH} peak moves toward higher bias. Further, the relative magnitude of the current peaks changes, with the V_p^{LH} peak becoming relatively stronger [compare with Fig. 1(b)]—indicative of shifts in the energy alignment of the 2D subbands with respect to the occupied emitter states. Since the V_p^{LH} shifts to lower bias, parasitic series resistance is not the cause. Further, for the device sizes D in Fig. 2, geometric lateral quantization energy scale $\hbar^2/2m^*D^2 \ll 1$ meV and hence cannot play any role. Therefore, the changing $I(V)$ characteristics of submicrometer RTDs can be unambiguously attributed to strain relaxation in the quantum well,[4] which reduces the subband separation ΔE_{00} and hence the V_p^{HH} and V_p^{LH} peak separation.

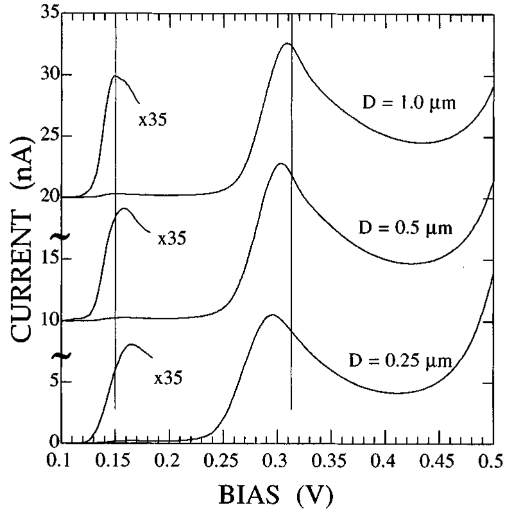

FIG. 2. (a) $I(V)$ characteristics of $D=1.0$, 0.5, and 0.25 μm devices. The current scale corresponds to the smallest device, other curves rescaled and shifted for clarity. The vertical lines indicate the V_p^{HH} and V_p^{LH} peak positions in large devices.

The measured resonant peak spacing shift $\Delta V_p \equiv (V_p^{\mathrm{LH}} - V_p^{\mathrm{HH}})$ for devices down to $D=0.20$ μm is shown in Fig. 3, together with the corresponding ΔE_{00} values obtained from the self-consistent calculations analogous to Fig. 1(c). If we assume that changes in the band-edge splitting ΔE translate directly into changes in the HH$_0$–LH$_0$ subband energy spacing ΔE_{00} and replace the nonuniform strain in the device by an average value, we can easily estimate the average strain

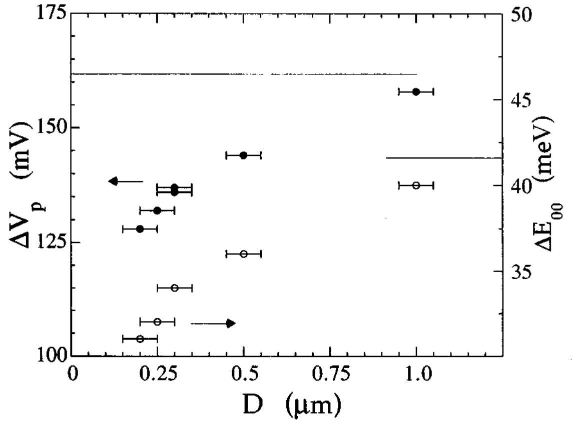

FIG. 3. Measured $I(V)$ peak separation (filled circles) and calculated HH$_0$–LH$_0$ energy separation ΔE_{00} (open circles) vs nominal device size D. Horizontal lines represent the large device result.

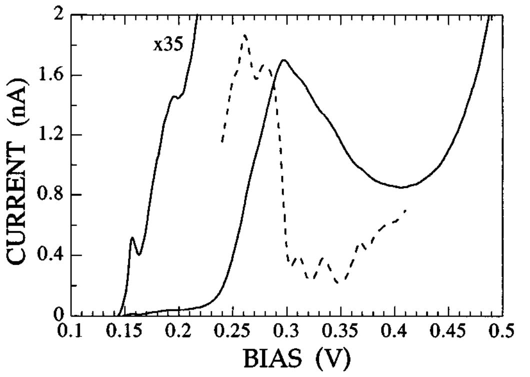

FIG. 4. $I(V)$ curve of the $D=0.1$ μm device at $T=1.5$ K. Note the additional fine structure in the V_p^{LH} peak, more easily seen in the dI/dV data (dashed line).

relaxation as a function of device size. The strain-induced band-edge splitting ΔE for $\mathrm{Si}_{1-x}\mathrm{Ge}_x$ strained to Si is given by[11]

$$\Delta E=\frac{[3\xi(x)+\Lambda(x)]-\sqrt{9\xi^2(x)+\Lambda^2(x)-2\xi(x)\Lambda(x)}}{2}, \qquad (1)$$

where $\Lambda(x=0.25)=0.106$ eV is the interpolated spin-orbit splitting, and $\xi(x)=29$ meV is the strain energy due to lattice mismatch. In bulk $\mathrm{Si}_{0.75}\mathrm{Ge}_{0.25}$, $\Delta E=40$ meV, whereas from Fig. 3 we find that in the $D=0.25$ μm device, the HH_0–LH_0 subband separation ΔE_{00} has decreased by -10 meV. Equation (1) then gives an average relaxation $\Delta\xi(x)\approx 9$ meV, about 30% of the strain energy in the $\mathrm{Si}_{0.75}\mathrm{Ge}_{0.25}$ layer on Si.

We stress that in addition to the naiveté of our model, the above estimate yields only an average value, whereas the actual strain energy distribution should be strongly nonuniform. Figure 4 shows the $T=1.5$ K $I(V)$ characteristics of the smallest successful device fabricated thus far ($D=0.1$ μm). The different overall line shape of the $I(V)$ resonant peaks makes comparison with the larger microstructures of Fig. 2 difficult. The V_p^{HH} peak has given way to a double steplike structure, while the stronger V_p^{LH} peak has developed an additional fine structure. We note once again that even for $D=0.1$ μm, the geometric lateral quantization energy scale is much too small to account for the observed structure. However, if the relatively sharp lateral distributions of strain energy calculated for narrow wires in Ref. 4 also holds for our dotlike structures, the quantization due to strain-induced ~10 meV lateral potential steps[20] would be consistent with the $I(V)$ curve shown in Fig. 4. The fabrication and measurement of more devices in the $D\sim 0.1$ μm regime is in progress.

In conclusion, we have used double-barrier resonant tunneling spectroscopy as a novel tool for examining strain relaxation in semiconductor microstructures. Our results indicate that strain relaxation is a large effect in submicrometer devices, reaching ~30% of the strain energy in $\mathrm{Si}_{0.75}\mathrm{Ge}_{0.25}$ layers when the lateral extent falls below 0.3 μm. Consequently, the properties of semiconductor devices with built-in strain calculated under the assumption that the strain remains unaffected by the fabrication of submicron structures may require re-examination.

One of the authors (A. Z.) has benefited greatly from a joint study agreement with T. P. Smith III of IBM Research. The work at Brown has been supported by the NSF Materials Research Group (Grant No. DMR-9121747) and ONR Young Investigator Program (Grant No. N00014-95-1-0729).

[1] See, for example, *Quantum Well Lasers*, edited by P. S. Zory (Academic, Boston, 1993).

[2] G. L. Bir and G. E. Pikus, *Symmetry and Strain-Induced Effects in Semiconductors* (Wiley, New York, 1974).

[3] S. Luryi and E. Suhir, Appl. Phys. Lett. **49**, 140 (1986).

[4] T. J. Gosling and J. R. Willis, J. Appl. Phys. **77**, 5601 (1995).

[5] This difficulty can be avoided by introducing a third material to confine the microstructure electronically and yet maintain in-plane strain uniformity; e.g., T. Yamauchi, T. Takahashi, J. N. Shulman, and Y. Arakawa, IEEE J. Quantum Electron. **29**, 2109 (1993).

[6] A review of $\mathrm{Si/Si}_{1-x}\mathrm{Ge}_x$ heterostructures in semiconductor devices is given in J. C. Bean, Proc. IEEE **80**, 571 (1992).

[7] H. C. Liu, D. Landheer, M. Buchanan, and D. C. Houghton, Appl. Phys. Lett. **52**, 1809 (1988).

[8] K. L. Wang, R. P. Karunasiri, J. Park, S. S. Rhee, and C. H. Chern, Superlattices Microstruct. **5**, 201 (1989).

[9] U. Gennser, V. P. Kesan, S. S. Iyer, T. J. Bucelot, and E. S. Yang, J. Vac. Sci. Technol. B **9**, 2280 (1991).

[10] G. Schuberth, G. Abstreiter, E. Gornik, F. Schäffler, and J. F. Luy, Phys. Rev. B **43**, 2280 (1991).

[11] R. People, Phys. Rev. B **32**, 1405 (1985).

[12] A. Zaslavsky, D. A. Grützmacher, Y. H. Lee, W. Ziegler, and T. O. Sedgwick, Appl. Phys. Lett. **61**, 2872 (1992).

[13] A. Zaslavsky, D. A. Grützmacher, S. Y. Lin, T. P. Smith III, R. A. Kiehl, and T. O. Sedgwick, Phys. Rev. B **47**, 16036 (1993).

[14] The processing steps are analogous to those employed in the three-terminal DBRT transistor fabrication reported in A. Zaslavsky *et al.*, Appl. Phys. Lett. **64**, 1699 (1994).

[15] S. Luryi, Appl. Phys. Lett. **47**, 490 (1985).

[16] Using the HETMOD software package written by A. C. Warren of IBM Research.

[17] E. E. Mendez, W. I. Wang, B. Ricco, and L. Esaki, Appl. Phys. Lett. **47**, 415 (1985).

[18] R. K. Hayden, L. Eaves, M. Henini, D. K. Maude, J. C. Portal, and G. Hill, Appl. Phys. Lett. **60**, 1474 (1992).

[19] E. P. O'Reilly and G. P. Witchlow, Phys. Rev. B **34**, 6030 (1985).

[20] Quantum confinement by lateral strain gradients created by depositing carbon stressors in GaAs quantum well material was reported in K. Kash *et al.*, Phys. Rev. Lett. **67**, 1326 (1991).